Available online at www.sciencedirect.com

SciVerse ScienceDirect

Ceramics International 38 (2012) 1635–1641

CERAMICS INTERNATIONAL

www.elsevier.com/locate/ceramint

Chemical composition evolution of YAG co-precipitate determined by pH during aging period and its effect on precursor properties

Yuanhua Sang [a], Yaohui Lv [b], Haiming Qin [a], Xiaolin Zhang [a], Hong Liu [a,*], Jiyang Wang [a], Xudong Sun [c], Robert I. Boughton [d]

[a] State Key Laboratory of Crystal Materials, Shandong University, 27 Shandanan Road, Jinan 250100, China
[b] School of Materials Science and Engineering, Anhui Key Laboratory of Metal Materials and Processing, Anhui University of Technology, Maanshan 243002, China
[c] School of Materials and Metallurgy, Northeastern University, Shenyang 110004, China
[d] Center for Material Science, Bowling Green State University, Bowling Green, OH 43403, USA

Received 21 July 2011; received in revised form 22 July 2011; accepted 14 September 2011
Available online 5 October 2011

Abstract

The properties of YAG precursors aged at various pH levels for different aging times were examined to explore the influence of pH on the evolution of the chemical composition and the morphology of the precipitate, on the variation of phase composition during the calcination process. Precursors obtained at pH lower than 8.0 can be transformed into mono-phase YAG by calcination at low temperature, while those obtained at higher pH exhibit a variety of crystalline structures. Aging at high pH increased the impurity content of the calcined powder. Based on monitoring the pH during the precursor aging process, and the measurement of the Y/Al ratio in the precipitates, the mechanism of the chemical variation is discussed and the influence of pH and aging time on the synthesis of YAG precursor is discussed.

Keywords: YAG precursor; Y/Al ratio; Phase transformation; Morphology

1. Introduction

Neodymium-doped yttrium aluminum garnet ($Y_{3-x}Nd_xAl_5O_{12}$) is one of the most important materials for use in laser applications. Since the first demonstration of Nd:YAG ceramic laser oscillation in 1995 by Ikesue et al. [1], significant progress has been made in the preparation of transparent YAG ceramic and YAG ceramic lasers. Much effort has been devoted to the development of synthesis methods and to controlling the synthesis process of YAG ceramic powder, in order to improve the ceramic quality. Many kinds of wet chemical synthesis routes are used in the preparation of fine powder for ceramics fabrication, such as numerous sol–gel methods [2,3], homogeneous precipitation [4,5], microwave irradiation [6,7], solvothermal [8,9] and supercritical water synthesis [10–12]. Most importantly, the co-precipitation method with ammonium hydrogen carbonate (AHC) as precipitant proposed by Yanagitani et al. [13–15] has become one of the most widely used routes for the synthesis of YAG nanopowder, because this low cost and mass-produced synthesis route can generate YAG powder with excellent dispersion and sintering properties [16–19]. In order to obtain high quality YAG powder, many parameters need to be carefully controlled during the synthesis process. Such parameters as reaction temperature [20], terminal pH value [21], duration of aging [6,19,22], dosage of ammonium sulfate [23], etc., need to be optimized because they are all interdependent during the formation and evolution of the precursor. The parameters produce complicated effects on the chemical composition and morphology, affecting the final properties of the precursor. The influence of pH and aging time of the precursor suspension has been widely investigated during the individual preparation of Al_2O_3 [24] and Y_2O_3 [25,26] powder via the precipitation method. The great influence of these parameters on the morphology and chemical composition of the yttria and alumina precursors, as well as on crystalline

* Corresponding author. Tel.: +86 531 88362807.
E-mail address: hongliu@sdu.edu.cn (H. Liu).

0272-8842/$36.00
doi:10.1016/j.ceramint.2011.09.054

evolution during the calcination process has been demonstrated. For the preparation of YAG powder, the previously widely held opinion on pH control is to provide a relatively stable pH between 8 and 9 with excess precipitant [20,27–29], assuming that would result in the yttrium and aluminum compounds precipitating simultaneously and homogenously with a favorable elemental distribution. However, the advantage of a relatively low pH has been observed by researchers [30], although the variation of the pH is significant during the reaction process. The effect of pH on the variation in the (Nd + Y):Al ratio of Nd:YAG nanopowder was demonstrated by Liu et al. [21]. On the other hand, the aging process is essential for the preparation of the YAG precursor in the precipitation process [6,30]. Different aging times (from 1 h to 72 h) have been used for the synthesis of the precursor, but the fundamental reason for the chosen has not been discussed.

Therefore, an in-depth understanding of the chemical and physical processes that occur during the preparation of YAG precursors has become necessary. In this work, the chemical composition (Y/Al ratio) and the morphology of YAG precursors aged at different pH were examined in order to investigate the evolution of the precursor during aging. The transformation of crystalline phases and the morphology of YAG powder with calcination were characterized for further understanding. A description of the mechanism governing the pH value during the aging process and its effect on the composition and morphology evolution in YAG precursors is proposed.

2. Experimental procedures

Y_2O_3 (Alfa Aesar, 99.99% purity) and $Al(NO_3)_3{\cdot}9H_2O$ (Alfa Aesar, 99.99% purity) were dissolved in HNO_3 and deionized water with ion concentration of 0.4 mol/L, respectively. These solutions were mixed corresponding to $Y_3Al_5O_{12}$ for synthesis of YAG precursors. Precipitant solution with concentration of 2 mol/L and pH = 8.45 was obtained by dissolving NH_4HCO_3 (Sinopharm Chemical Reagent Co., Ltd., AR) in deionized water. The YAG precipitates were obtained by adding the mixed solutions to the precipitant through reversed titration process, titration suspended at different pH from 6.00 to 7.30. The precipitate samples were derived from 2 mL of different suspension samples, including: at the titration suspension point, after aging for 25 min with agitation, after aging for 150 min with agitation, after aging for 12 h without agitation, as well as precursors taken after washing and drying. To infer the compounds in the YAG precursor, individual Y_2O_3 and Al_2O_3 precursors were synthesized via the titration method at low and high pH. After filtration, washing and drying, the precursor samples were calcined at different temperatures ranging from 550 to 1300 °C for 3 h to check for phase transformation. The YAG precursor synthesized at the lowest pH (6.0) was also calcined at temperatures between 820 °C and 960 °C at a heating rate of 5 °C/min and dwelled 5 min at each temperature point to investigate phase evolution. Precursors prepared at the highest pH (7.3) with and without aging were calcined at 1200 °C for 3 h to study the effect of aging on phase evolution.

The pH of the suspension was monitored with a pH meter with an accuracy of 0.02 (PHS-3D, Leici, China). The chemical compositions (Y/Al ratios) of all the precipitate samples were checked to explore the effect of aging time on the precursor's chemical composition evolution with an inductively coupled plasma emission spectrometer (ICP-AES, IRIS Intrepid II XSP, Thermo Electron Corporation, USA). X-ray diffraction (XRD) data were recorded using Cu K_α (1.5406 Å, 1.5444 Å), 6°/min with D8-advance, Germany. Transmission electron microscope (TEM) images were taken on a JEM transmission electron microscope (Japan Electronics Co., Ltd.). Field emission scanning electron microscope (FESEM) images and energy-dispersive X-ray spectroscopy (EDS) of the samples were taken on a Hitachi S-4800 high-resolution scanning electron microscope.

3. Results and discussion

3.1. Chemical composition variation of the precursors during the aging period

Samples and the related pH values at different points in the aging period are listed in Table 1. Samples s1–s7 are defined by the pH of the reaction systems at the following titration suspension points: 6.00, 6.15, 6.30, 6.45, 6.75, 7.10, and 7.29, respectively. After 25 min of aging, the pH of the reaction system greatly increases, up to: 6.89, 7.10, 7.23, 7.42, 7.63, 7.72, and 7.94, respectively. After aging for 150 min, the pH of the reaction system approaches a limiting value, and the final pH values are: 7.28, 7.51, 7.65, 7.85, 8.09, 8.30, and 8.42, respectively. This evolution of pH is consistent with results reported earlier [31]. After aging for 12 h, the pH of the reaction

Table 1
Samples and the related pH values at different reaction points.

Samples	pH values			
	Titration terminal point	25 min aging with agitation	150 min aging with agitation	12 h aging with settlement
s1	6.00	6.89	7.28	7.26
s2	6.15	7.10	7.51	7.48
s3	6.30	7.23	7.65	7.65
s4	6.45	7.42	7.85	7.83
s5	6.75	7.63	8.09	8.05
s6	7.10	7.72	8.30	8.23
s7	7.29	7.94	8.42	8.44

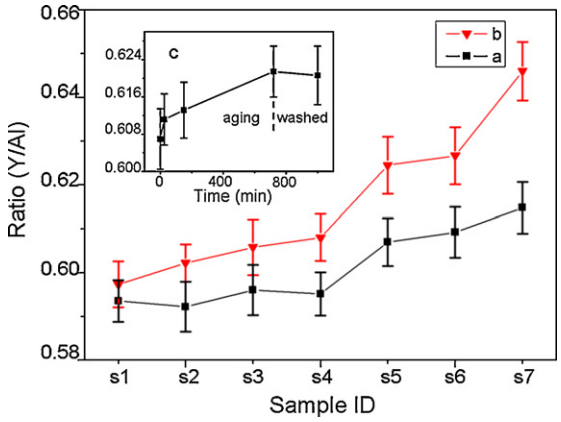

Fig. 1. Y/Al ratio of the samples after aging for different time measured by ICP-AES. The variation of the Y/Al ratios among the samples obtained at the titration suspended points (a) and aging for 12 h without agitation (b). The detail Y/Al ratio variation of sample s5 different points (c).

system changes very slightly, this indicates that the system becomes stable after aging for 150 min.

As reported, Al-precipitate [24] and Y-precipitate [25,26] should be formed as hydrous aluminum and hydrous yttrium with amorphous structures. With aging, carbonate ions (CO_3^{2-}) exchange moieties with H_2O molecules, constrict the structures, and form better-crystallized precursors with the hydroxide ions. Constraint by the amount of NH_4HCO_3 present, the final product varies from AlOOH to $NH_4Al(OH)_2CO_3{\cdot}xH_2O$ in the Al-precipitate case, and from $Y_2(CO_3)_3{\cdot}xH_2O$ to $Y(OH)CO_3{\cdot}xH_2O$ in the Y-precipitate case. For the synthesis of the YAG precursor, the previous compound formed in the reaction system should be a mixture of hydrous aluminum and yttrium, especially for synthesis at a low pH value. After aging process, the preferable compositions of a mixture of $NH_4Al(OH)_2CO_3{\cdot}xH_2O$ and $Y_2(CO_3)_3{\cdot}xH_2O$ formed as reported by Li et al. [19,32].

The Y/Al ratios of the samples after aging for different times measured by ICP are shown in Fig. 1. Fig. 1a and b shows the variation of the Y/Al ratios among the samples obtained at the titration suspension point and after aging for 12 h without agitation, respectively. At first, the pH of samples s1–s4 lie in the range of 6.0–6.45, and the Y/Al ratio is slightly less than 0.6 (Fig. 1a). With the increase in the pH, the Y/Al ratios of samples s4–s7 clearly increase. This phenomenon might be caused by the accomplishment of yttrium with the increase of pH. The Y/Al ratios increase (Fig. 1b), especially the one aging at higher pH. A significant increase in the Y/Al ratio is observed between samples s4 and s5. This phenomenon is considered to be the result of redissolution of Al precipitate at the pH around 8.09, and higher pH increases the redissolution of Al precipitate. The process for the redissolution is still uncertain, however, the result is consistent with the results reported by Liu et al. [21]. Fig. 1c illustrates the detailed Y/Al ratio variation of sample s5 as a typical representation of the other samples. A rapid increase in the Y/Al ratio occurs at the beginning of aging, due to the rapid increase of the pH from 6.75 to 7.63, which is related to the accomplishment of precipitation. Then the Y/Al ratios of the sample increase linearly, implying the redissolution of Al precipitate is stable.

3.2. Phase transformation by calcination

Fig. 2 shows the XRD patterns of the samples calcined at 1300 °C for 3 h. Samples s1–s4 are pure YAG phases (JCPDS card No. 72-1315), while some impure phases appear in samples s5–s7. The main impure phase is $Y_4Al_2O_9$ (abbreviated to YAM, JCPDS card No. 78-2429), while even Y_2O_3 (JCPDS card No. 79-1256) is detected in sample s7.

The phase transformation of the samples calcined at various temperatures is shown in Fig. 3. Fig. 3a illustrates the crystalline phase evolution of sample s1, which was prepared at the lowest pH value (titration suspended at a pH of 6.0, and aging at a pH of 7.26). Fig. 3b shows the evolution of sample s7, which was synthesized at the highest pH value (titration suspended at a pH of 7.3 and aging at a pH of 8.44). The XRD results for sample s7 calcined at 1200 °C for 3 h (prepared with and without the aging process) are shown in Fig. 3c.

No crystalline structure appears after calcination at temperatures below 860 °C for 5 min (Fig. 3a). A mono-phase of hexagonal $YAlO_3$ (abbreviated to YAH, JCPDS card No.74-1334) appears when the calcination temperature is raised to 860 °C. The first formation of a YAG crystal structure is detected in the sample calcined at 900 °C. With an increase in calcination temperature, peaks related to the YAH phase decrease, while peaks related to the YAG phase increase, which indicates that YAH continuously transforms into YAG by

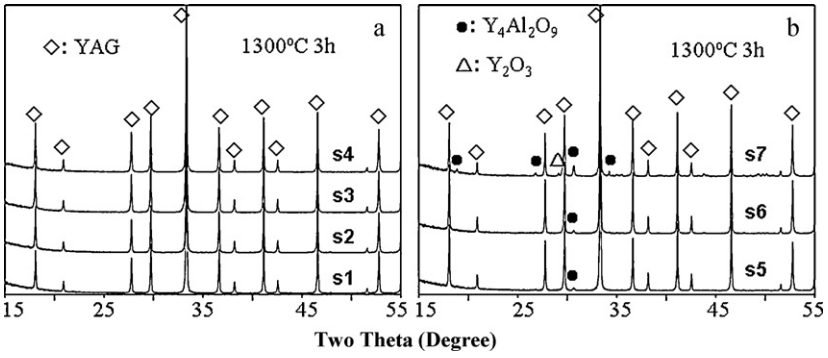

Fig. 2. XRD patterns of the samples calcined at 1300 °C for 3 h.

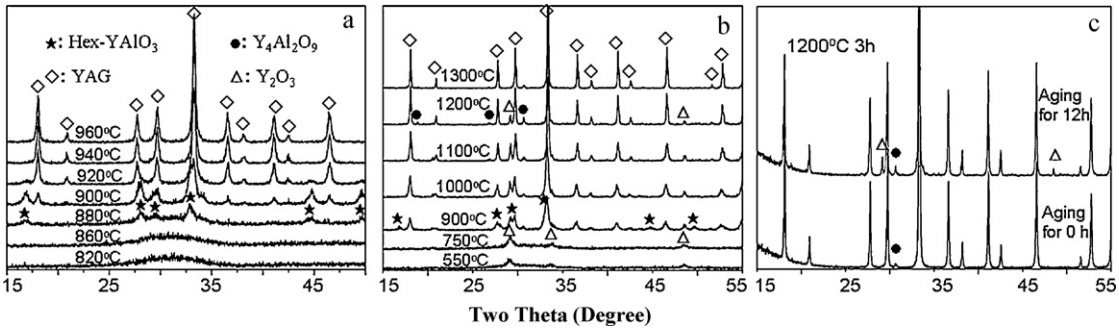

Fig. 3. Samples calcined at various temperatures. The crystalline phase evolution of sample s1 (a) and sample s7 (b), and sample s7 prepared with and without aging process calcined at 1200 °C for 3 h (c).

reaction with weakly crystalline Al_2O_3 in the temperature range from 860 °C to 940 °C. When the calcination temperature is raised above 940 °C, the peaks related to the YAG sharpen, corresponding to the improvement in the YAG crystallization.

As shown in Fig. 3b, the formation of YAG phases is more complex. The first crystalline phase detected in sample s7 at 550 °C is cubic Y_2O_3, and the crystallization temperature is about 300 °C lower than that of sample s1. The YAH and YAG phases as well as a small amount of the YAM phase are detected at 900 °C. With the temperature increase, the YAH phase disappears as in sample s1, and forms the mixture of YAG, YAM and Y_2O_3. The main YAG phase with a small amount of YAM is detected in the sample without aging, while the YAG phase with YAM and Y_2O_3, is detected in the sample that was aged for 12 h (shown in Fig. 3c).

Considering the difference in the ion product constants for yttrium and aluminum, the distribution of Al and Y is not ideal in the precipitate. Elemental diffusion is necessary during the calcination reaction, so the transitional structure of the YAH phase cannot be skipped during the phase transformation.

Calcination of the mono-Al-precipitate below 1000 °C produces weak crystallized Al_2O_3, while the mono-Y-precipitate readily forms in a crystalline structure with calcination at 550 °C (Supplement Table 1). The precursor of sample s1 is likely to interact as soon as it decomposes, and forms non-crystalline compounds, so no individual phase, especially the Y_2O_3 phase, is detected in the products by calcination at the low temperature. This phenomenon implies that yttrium and aluminum are well distributed in the precursor to react with each other. By contrast, the appearance of a single Y_2O_3 phase in sample s7 indicates obvious separation of the Y-precipitate from the Al-precipitate in the precursor, and some decomposed products do not react with each other, leaving the elements crystallizing to form the Y_2O_3 phase in a normal way. Although Al_2O_3 is not detected in any of its weakly crystalline structures, the appearance of YAM at 900 °C demonstrates the co-existence of crystalline Al_2O_3 and Y_2O_3, because it is consistent with the typical solid-state reaction process [33]. However, the large amount of YAG and YAH detected in the sample indicates that a composition similar to that of sample s1 forms the main part of the precursor. As shown in Fig. 3c, the existence of the YAM phase in the sample without aging is most likely induced by a non-homogenous elemental distribution in the previous product, which has aged during titration at a relatively high pH value. However, the appearance of Y_2O_3 in the sample after aging indicates an increase in non-homogeneity. This result provides direct evidence for the change of the precursor happens in the aging process. Combined with these results, we conclude that the precipitate should have similar homogenous structures at first, and that compound division and chemical change take place during aging process at high pH.

3.3. Morphology

TEM micrographs of precursors after aging are shown in Fig. 4. Fig. 4a and b exhibits the morphology of Al-precipitates synthesized at low and high pH, respectively. A fibroid shaped precursor is generated at low pH, while it shows a granular morphology obtained at high pH. Fig. 4c and d shows the morphology of YAG precursors in samples s1 and s7, respectively. The precursor morphology of sample s1 consists of particles, while that of sample s7 includes particles and a flake-like precipitate. According to the morphology of Y-precipitates synthesized at both low and high pH (Fig. 4e), we deduce that the flakes in sample s7 are individual Y-precipitate. This result argues for the division of the Y-precipitate and Al-precipitate in precursor synthesized at high pH.

Fig. 5 exhibits SEM images of the precursors for samples s1 and s7, as well as the resultant powder calcined at 1300 °C for 3 h. Consistent with Fig. 4c and d, the morphology of sample s1 is particle-like (Fig. 5a), and that of sample s7 is a mixture of particles and flakes (Fig. 5b). After calcination at 1300 °C for 3 h, sample s1 forms well-crystallized particles in size of 200 nm with no evident agglomeration (Fig. 5c), while some agglomerate shows in sample s7 (Fig. 5d). Energy-dispersive X-ray spectroscopy (EDS) of sample s7 was taken in the rectangular zone at the location of the agglomerate (Fig. 5d). The result of the EDS is shown in Fig. 5e and indicates that the Y/Al ratio in the agglomerate is 0.77, a value that is about 28% higher than the stoichiometric ratio.

Our previous research confirmed that the Y/Al ratios during the titration process are statistically stable [31], which implied the co-precipitation process. Comparing the morphology of the individual Y- and Al-precipitates with the YAG precursor in sample s1, the co-precipitation process apparently prevents the Y- and Al-precipitates from forming the essential morphology, and produce particles with better homogeneity. A high pH

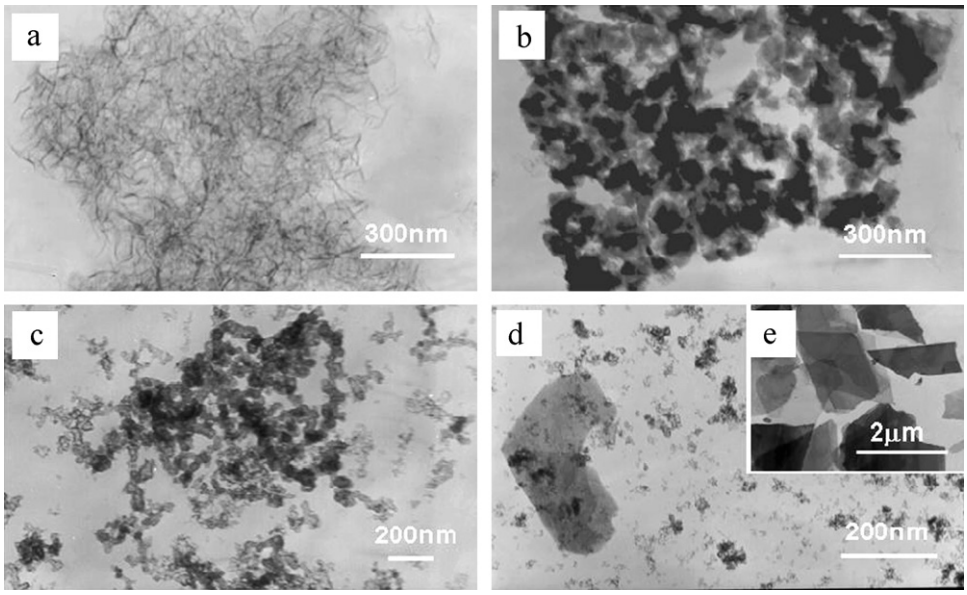

Fig. 4. TEM micrographs of the precursors with aging process, morphology of Al-precipitates synthesized at low (a) and high pH values (b), morphology of YAG precursors of sample s1 (c) and s7 (d), morphology of Y-precipitates synthesized at both low and high pH values (e).

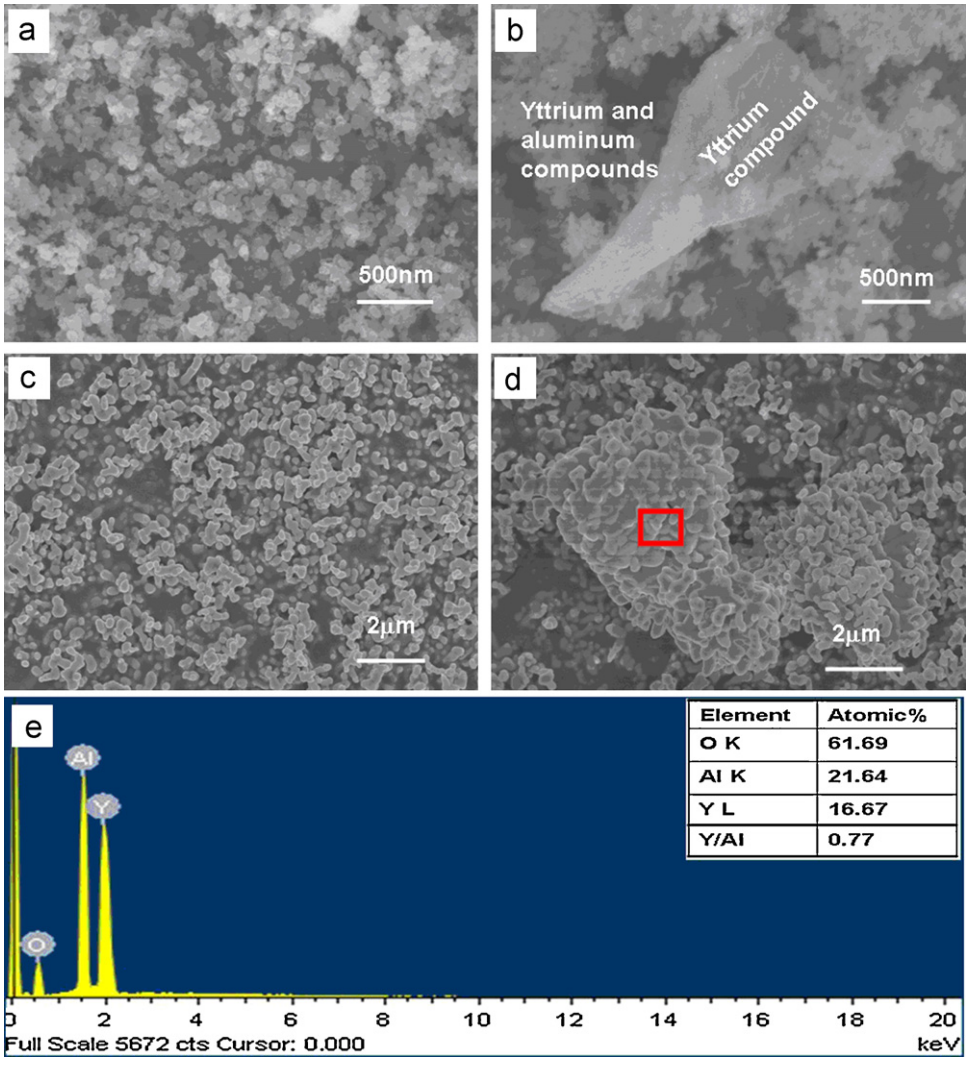

Fig. 5. SEM images of the precursors and the resultant powders calcined at 1300 °C for 3 h of samples s1 (a and c) and s7 (b and d), and the EDS result of the rectangle zone on the agglomerate (e).

would induce Al precipitate redissolution, and induce the yttrium compounds to reconstruct separately from the aluminum compounds. The local enrichment of yttrium leads to the formation of its normal flake-like morphology. The flake-like Y-precipitate crystallizes into Y_2O_3 with calcination, and makes the reaction the same as the solid-state reaction. The supplemental aluminum required for the reaction with yttrium is not sufficient around the big Y_2O_3 flakes in the powder state during calcination. The EDS result (0.77) invalidates any greater deviation of the chemical composition from the average value (0.64) of the system tested by ICP.

4. Conclusions

YAG precursors were synthesized at various pH levels. The effect of pH during the aging period was examined by investigating the Y/Al ratios, phase transformations, powder morphology. The results indicate that different composition and homogeneity in the precursor are caused by different pH during the aging process. When the pH is above 8, the redissolution of Al precipitate becomes significant, which leads to a complicated reaction process and impure phases during calcination. These problems would reduce the quality of the ceramic. The results of this study indicate that during the synthesis of the YAG precursor, the pH and aging duration should be carefully controlled. It is feasible to obtain a good quality transparent ceramic by aging with a pH value below 8 and a duration time of 12 h.

Acknowledgements

This research was supported by NSFC (NSFDYS: 50925205, Grant: 50990303, 50872070, IRG: 50721002 and 973 program: 2010CB833103) and 111 program No. b06015.

Appendix A. Supplementary data

Supplementary data associated with this article can be found, in the online version, at doi:10.1016/j.ceramint.2011.09.054.

References

[1] A. Ikesue, T. Kinoshita, K. Kamata, K. Yoshida, Fabrication and optical properties of high-performance polycrystalline Nd:YAG ceramics for solid-state lasers, J. Am. Ceram. Soc. 78 (1995) 1033–1040.
[2] S.A. Hassanzadeh-Tabrizi, E. Taheri-Nassaj, H. Sarpoolaky, Synthesis of an alumina-YAG nanopowder via sol–gel method, J. Alloys Compd. 456 (2008) 282–285.
[3] Y.P. Fu, S.B. Wen, C.S. Hsu, Preparation and characterization of $Y_3Al_5O_{12}$:Ce and Y_2O_3:Eu phosphors powders by combustion process, J. Alloys Compd. 458 (2008) 318–322.
[4] D.J. Sordelet, M. Akinc, M.L. Panchula, Y. Han, M.H. Han, Synthesis of yttrium aluminum garnet precursor powders by homogeneous precipitation, J. Eur. Ceram. Soc. 14 (1994) 123–130.
[5] J.G. Li, X.D. Li, X.D. Sun, T. Ikegami, T. Ishigaki, Uniform colloidal cpheres for $(Y_{1-x}Gd_x)_2O_3$ ($x = 0$–1): formation mechanism, compositional impacts, and physicochemical properties of the oxides, Chem. Mater. 20 (2008) 2274–2281.
[6] X.L. Zhang, D. Liu, Y.H. Sang, H. Liu, J.Y. Wang, Effects of aging on the characteristices of Nd:YAG nano-powders, J. Alloys Compd. 502 (2010) 206–210.
[7] M.L. Saladino, G. Nasillo, D.C. Martino, E. Caponetti, Synthesis of Nd:YAG nanopowder using the citrate method with microwave irradiation, J. Alloys Compd. 491 (2010) 737–741.
[8] X. Li, H. Liu, J.Y. Wang, F. Han, R.I. Boughton, Production of nanosized YAG powders with spherical morphology and nonaggregation via a solvothermal method, J. Am. Ceram. Soc. 87 (2004) 2288–2290.
[9] Z.G. Wu, X.D. Zhang, W. He, Y.W. Du, N.T. Jia, P.C. Liu, F.Q. Bu, Solvothermal synthesis of spherical YAG powders via different precipitants, J. Alloys Compd. 472 (2009) 576–580.
[10] J.H. In, H.C. Lee, M.J. Yoon, K.K. Lee, J.W. Lee, C.H. Lee, Synthesis of nano-sized YAG:Eu^{3+} phosphor in continuous supercritical water system, J. Supercrit. Fluids 40 (2007) 389–396.
[11] M. Danchevskaya, Y. Ivakin, S. Torbin, G. Muravieva, Technological capability of synthesis of inorganic oxides in water fluid in neighborhood of critical point, J. Supercrit. Fluids 46 (2008) 358–364.
[12] Q.X. Zheng, B. Li, H.D. Zhang, J.J. Zheng, M.H. Jiang, X.T. Tao, Fabrication of YAG mono-dispersed particles with a novel combination method employing supercritical water process, J. Supercrit. Fluids 50 (2009) 77–81.
[13] T. Yanagitani, H. Yagi, M. Ichikawa, Japanese patent: 10-101333 (1997).
[14] T. Yanagitani, H. Yagi, Y. Hiro, Japanese patent: 10-101411 (1998).
[15] H. Yagi, T. Yanagitani, K. Takaichi, K.I. Ueda, A.A. Kaminskiim, Characterization and laser performance of highly transparent Nd^{3+}:$Y_3Al_5O_{12}$ laser ceramics, Opt. Mater. 29 (2007) 1258–1262.
[16] H. Gong, D.Y. Tang, H. Huang, J. Ma, Agglomeration control of Nd:YAG nanoparticles via freeze drying for transparent Nd:YAG ceramics, J. Am. Ceram. Soc. 92 (2009) 812–817.
[17] Xia Li, Qiang Li, Jiyang Wang, Shunliang Yang, Hong Liu, Synthesis of Nd^{3+} doped nano-crystalline yttrium aluminum garnet (YAG) powders leading to transparent ceramic, Opt. Mater. 29 (2007) 528–531.
[18] A.K. Pradhan, K. Zhang, G.B. Loutts, Synthesis of neodymium-doped yttrium aluminum garnet (YAG) nanocrystalline powders leading to transparent ceramics, Mater. Res. Bull. 39 (2004) 1291–1298.
[19] J.G. Li, T. Ikegami, J.H. Lee, T. Mori, Y. Yajima, Co-precipitation synthesis and sintering of yttrium, aluminum garnet (YAG) powders: the effect of precipitant, J. Eur. Ceram. Soc. 20 (2000) 2395–2405.
[20] P. Palmeroa, C. Esnoufb, L. Montanaroa, G. Fantozzib, Influence of the co-precipitation temperature on phase evolution in yttrium-aluminium oxide materials, J. Eur. Ceram. Soc. 25 (2005) 1565–1573.
[21] W.B. Liu, W.X. Zhang, J. Li, H.M. Kou, Y.Q. Shen, L. Wang, Y. Shi, D. Zhang, Y.B. Pan, Influence of pH values on (Nd + Y):Al molar ratio of Nd:YAG nanopowders and preparation of transparent ceramics, J. Alloys Compd. 503 (2010) 525–528.
[22] M. Suarez, A. Fernandez, J.L. Menendez, M. Nygren, R. Torrecillas, Z. Zhao, Hot isostatic pressing of optically active Nd:YAG powders doped by a colloidal processing route, J. Eur. Ceram. Soc. 30 (2010) 1489–1494.
[23] J.Q. Wang, H.Y. Xu, Y. Wang, Y.L. Yue, Effect of sulfate ions on YAG powders synthesized by microwave homogeneous precipitation, J. Rare Earths 24 (2006) 284–287.
[24] X.L. Du, Y.Q. Wang, X.H. Su, J.G. Li, Influences of pH value on the microstructure and phase transformation of aluminum hydroxide, Powder Technol. 192 (2009) 40–46.
[25] L.Y. He, N.P. Li, Research on mechanism of preparation of crystalline yttrium carbonate by precipitation of ammonium bicarbonate, Rare Met. Cement. Carb. 30 (2002) 1–5.
[26] Z.G. Huang, X.D. Sun, Z.M. Xiu, S.W. Chen, C.T. Tsai, Precipitation synthesis and sintering of yttria nanopowders, Mater. Lett. 58 (2004) 2137–2142.
[27] H. Wang, L. Gao, K. Niihara, Synthesis of nanoscale yttrium aluminum garnet powder by the co-precipitation method, Mater. Sci. Eng. A 288 (2000) 1–4.
[28] W.Q. Li, L. Gao, Co-precipitation processed needle-like YAG dispersed in alumina powder, Mater. Lett. 48 (2001) 157–161.
[29] X. Li, H. Liu, J.Y. Wang, X.D. Zhang, H.M. Cui, Preparation and properties of YAG nano-sized powder from different precipitating agent, Opt. Mater. 25 (2004) 407–412.

[30] S. Nishiura, S. Tanabe, K. Fujioka, Y. Fujimoto, Properties of transparent Ce:YAG ceramic phosphors for white LED, Opt. Mater. 33 (2011) 688–691.
[31] Y.H. Sang, H. Liu, X.D. Sun, X.L. Zhang, H.M. Qin, Y.H. Lv, D. Huo, D. Liu, J.Y. Wang, R.I. Boughton, Foramation and calcination temperature-dependent sintering activity of YAG precursor synthesized via reverse titration method, J. Alloys Compd. 509 (2011) 2407–2413.
[32] J.G. Li, T. Ikegami, J.H. Lee, T. Mori, Y. Yajima, Reactive yttrium aluminate garnet powder via co-precipitation using ammonium hydrogen carbonate as the precipitant, J. Mater. Res. 15 (2000) 1864–1867.
[33] V.B. Gusshkova, V.A. Krzhizhanovskaya, O.N. Egorova, Interaction of yttrium and aluminum oxide, J. Inorg. Mater. 19 (1983) 80–84.